

Advanced Energy Management and Power Quality Enhancement in DC Micro-grids with EV Fast Charging Using ANN-Controlled STATCOM

Hachimenum Nyebuchi Amadi¹, Henry Okechukwu Williams², Richeal Chinaeche Ijeoma³ Department of Electrical and Electronics Engineering, Rivers State University, Port-Harcourt, Nigeria

Abstract- The rapid integration of electric vehicle (EV) fast charging stations in DC micro-grids has introduced significant power quality challenges, particularly harmonic current distortion at the point of common coupling (PCC). In this study, a DC microgrid integrating photovoltaic (PV) generation, battery energy storage systems (BESS), and a Level-3 EV fast charging station was modeled in MATLAB/Simulink to examine the effect of harmonic distortion and evaluate mitigation using an Artificial Neural Network (ANN)-controlled Static Synchronous Compensator (STATCOM). Base case simulation results revealed that the EV fast charging station injected excessive harmonic distortion into the network, with dominant odd harmonics at the 11th and 13th orders, leading to a total harmonic distortion (THD) of 14.05%. This value significantly exceeds the IEEE 519-2022 standard limit of 8% for medium-voltage systems. Following the installation of an ANN-tuned STATCOM at the PCC, the harmonic distortion was substantially mitigated, reducing the 11th and 13th orders to 0.01% and 0.15% respectively. Consequently, the total harmonic distortion was minimized to 1.23%, achieving a 91.24% reduction and ensuring full compliance with IEEE standards. Furthermore, the ANN controller demonstrated excellent training performance with a best validation mean square error of 0.0034611 at epoch 20 and a regression correlation coefficient of R = 0.9879, validating its accuracy and robustness. These findings confirm that ANN-controlled STATCOM provides an effective and intelligent solution for enhancing power quality and system stability in DC micro-grids with EV fast charging integration.

Keywords – DC micro-grid; Electric vehicle fast charging; ANN-controlled STATCOM; Harmonic mitigation; Power quality.

I. INTRODUCTION

Recent technological advances and the anticipated economic and environmental benefits of electrified transport have significantly accelerated the adoption of electric vehicles (EVs). According to the International Energy Agency (IEA), the global EV fleet is projected to reach nearly 250 million by 2030. This trend, while promising for sustainable development, poses major challenges for existing power systems, especially in the context of EV charging infrastructure. Traditional EV charging units Level 1 and Level 2 require between 4 to 16 hours to fully charge a battery, making them impractical for scenarios requiring fast turnaround. To address this limitation, Level-3 DC fast charging units have emerged, capable of charging an EV in less than 30 minutes. However, the deployment of EV fast charging stations (EVCS) introduces significant technical concerns. These units impose high instantaneous power demand, which can stress the distribution network, increase carbon emissions when powered from conventional grids, and contribute to voltage fluctuations, harmonic distortion, and power losses. The situation is even more critical at the residential and community distribution

level, where such chargers are directly connected to relatively weak networks. To mitigate these impacts, DC micro-grids integrating renewable energy sources (RES) and energy storage systems (ESS) have gained attention as a viable solution for supporting EV fast charging. Yet, the dynamic and nonlinear characteristics of EVCS still pose power quality and energy management challenges. Flexible AC Transmission System (FACTS) devices, particularly the Static Synchronous Compensator (STATCOM), are effective in regulating voltage, providing reactive power support, and improving power quality. Nevertheless, the effectiveness of STATCOM depends on its control strategy. Conventional proportional—integral (PI) controllers are limited under rapidly varying load and renewable conditions.

Artificial Neural Network (ANN)-based control presents a promising alternative due to its adaptive and data-driven capabilities. ANN-controlled STATCOMs can enhance microgrid stability, reduce harmonic distortion, and ensure optimal energy management under the complex and nonlinear dynamics of EV fast charging. This motivates the need to explore ANN-based STATCOM control for advanced energy



Volume 11, Issue 4, Jul-Aug-2025, ISSN (Online): 2395-566X

management and power quality enhancement in DC microgrids with EV fast charging integration.

The increasing penetration of distributed generation (DG) and electric vehicle (EV) fast charging in modern grids has created complex challenges in stability, control, and power quality management. Various control strategies and compensation devices have been proposed in the literature to address these challenges. Electrical power systems are designed to provide consistent and reliable voltage to end users. Accurately predicting future energy demand is crucial for effective planning of power generation, distribution, and infrastructure development to meet the anticipated needs of the community (Ijeoma and Odu, 2025a). Electricity can be generated in various types of power plants, including thermal, hydroelectric, and nuclear facilities. Once generated, the electricity is supplied to a transmission substation located near the power plant. At this substation, the voltage is significantly increased using step-up transformers. This increase in voltage helps to minimize transmission losses over long distances (Ijeoma and Olisa, 2019).

Mwasilu and Ojo (2024) highlight the limitations of voltage-sourced converters (VSCs) in grid-connected DG systems, particularly their interaction with LCL filters, which can trigger resonance issues and compromise stability. Their proposed robust multi-input multi-output (R-MIMO) controller mitigates high-frequency switching harmonics and improves reliability without the need for additional damping mechanisms. This advancement emphasizes the importance of intelligent control strategies for stability under diverse operating conditions.

Shravani et al. (2023) investigate the mitigation of harmonics generated by nonlinear loads. Their study demonstrates the effectiveness of active power conditioners, such as Shunt Active Power Filters (SAPFs) and Unified Power Quality Conditioners (UPQCs), especially when combined with renewable energy sources. While simulations confirm the benefits, the study highlights the gap in real-world implementation, pointing to the need for robust controllers that adapt to dynamic grid conditions.

Altin et al. (2023) propose a multi-agent control system for DC micro-grids integrating photovoltaics, wind, storage, and synchronous generation. Their results confirm the ability of multi-agent frameworks to stabilize DC bus voltage and ensure effective energy management. However, their scope remains limited to a few operational scenarios, leaving open questions about scalability and adaptability in EV-integrated DC microgrids.

Bianchi and Medici (2017) explore Proportional-Integral-Derivative (PID) controllers in DG systems, noting their simplicity and effectiveness in stable environments but also their weaknesses in highly nonlinear, dynamic systems such as those influenced by EV fast charging. Tuan and Wang (2018) advance this discussion by demonstrating that fuzzy logic control (FLC) can handle uncertainty in renewable-based DG systems, although rule construction becomes increasingly complex for larger networks. Just as the continuous flow of blood is essential for human survival, a stable and reliable supply of electricity is fundamental to national development. Without electricity, no city or nation can thrive (Fubara and Ijeoma, 2019). Innovative energy practices and solutions offer a clear pathway to uplifting communities worldwide. By prioritizing localized energy systems, adopting renewable technologies, enhancing energy efficiency, and fostering inclusive policies, we can create a world where energy access is not a privilege but a fundamental right (Ijeoma, 2025c).

Zhao and Xu (2019) show that Model Predictive Control (MPC) optimizes power dispatch in hybrid DG systems by predicting future states, though its computational burden remains a barrier for real-time EV applications. Similarly, Pan and Wang (2018) emphasize the effectiveness of adaptive control in handling time-varying dynamics, but note implementation challenges in large-scale systems.

Liu and Li (2019) complement this with the use of Sliding Mode Control (SMC), which demonstrates robustness to disturbances but introduces chattering effects that can limit practical deployment.

Huang and Tang (2017) employ Genetic Algorithms (GA) and Particle Swarm Optimization (PSO) to optimize renewable integration, while Mir Nahidul Ambia et al. (2015) apply Harmony Search Algorithm (HSA) to improve controller performance. Both approaches highlight strong adaptability but face computational challenges and limited real-world validation.

Zhou and Yu (2020) present hybrid control strategies, such as FLC-PID or MPC combinations, to balance multiple objectives in DG systems, while Zhou and Zhang (2020) explore VSC-based voltage and reactive power control for stable renewable integration.

Zhang and Wang (2019) further extend this by proposing Unified Power Quality Conditioners (UPQCs) to tackle multiple power quality issues simultaneously, though their high cost and complexity limit scalability.

Razmi and Lu (2022) provide a comprehensive review of Model Predictive Control in microgrid applications, stressing the importance of hierarchical strategies for distributed energy resource management but identifying gaps in real-world validation.

Hong et al. (2019) contribute to this by introducing an integrated three-port converter for PV/battery hybrid systems, which improves efficiency and reduces hardware complexity through coordinated energy management.

Overall, the literature reveals a progression from traditional PID-based control toward intelligent, adaptive, and



Volume 11, Issue 4, Jul-Aug-2025, ISSN (Online): 2395-566X

optimization-driven strategies aimed at enhancing stability, power quality, and energy management in microgrids. However, gaps remain in simultaneously addressing power quality disturbances from EV fast charging and energy management in DC microgrids. While STATCOM devices have proven effective for reactive power compensation and harmonic mitigation, their performance is often constrained by classical PI controllers. This gap motivates the present study, which introduces an ANN-controlled STATCOM designed to provide adaptive, real-time compensation for voltage fluctuations and harmonics while coordinating energy management in DC microgrids with EV fast charging

Review of Artificial Neural Network

Artificial Neural Networks (ANNs) are computational models inspired by the structure and function of the human brain. They consist of interconnected processing units, or neurons, organized in layers that process information in a parallel and distributed manner. Similar to biological synapses, these artificial neurons transmit signals through weighted connections, with each neuron's output determined by a nonlinear function of its inputs. A typical ANN architecture includes three main layers: the input layer, which receives external signals; one or more hidden layers, which perform nonlinear transformations; and the output layer, which produces the final response (Madueme and Kalu, 2015).

ANNs are particularly powerful because of their ability to learn from examples. During the learning phase, the network modifies its connection weights in response to training data, enabling it to capture complex patterns and relationships. This adaptive learning process makes ANNs suitable for applications such as fault detection, stability analysis, load forecasting, and harmonic mitigation in power systems. Their strength lies in their capacity to generalize knowledge beyond the training data, allowing them to handle dynamic and uncertain environments effectively.

Learning Techniques in Neural Networks

The ability of ANNs to learn depends on the training algorithm employed. Broadly, ANN learning techniques fall into three categories: supervised learning, unsupervised learning, and reinforcement learning. Each has unique characteristics and applications

• Supervised Learning

Supervised learning is the most common paradigm, where the network is trained using input—output pairs. The algorithm adjusts its internal weights to minimize the error between predicted and actual outputs. This process often employs the backpropagation algorithm, where errors are propagated backward to refine the model iteratively (Mohan et al., 2019). Supervised learning is effective in power system applications with well-defined datasets, such as load forecasting or fault

classification. However, its performance relies heavily on the quality and diversity of training data

• Unsupervised Learning

In contrast, unsupervised learning operates without labeled outputs. Here, the ANN identifies hidden patterns or correlations in the input data. Techniques such as clustering and dimensionality reduction are commonly used to group similar data points or extract essential features for analysis (Stuart and Peter, 2015). This paradigm is particularly useful in exploratory applications such as anomaly detection, load profile clustering, or uncovering consumption patterns in smart grids, where predefined target outputs are unavailable

• Reinforcement learning

Finally, reinforcement learning (RL) enables ANNs to learn through interaction with an environment. The system makes decisions and receives feedback in the form of rewards or penalties, gradually learning to maximize cumulative rewards (Stuart and Peter, 2015). This approach is valuable in dynamic and uncertain scenarios such as microgrid energy management, where the ANN must adapt to real-time fluctuations in demand and generation. Although promising, RL can be computationally intensive and requires careful design to ensure stability and convergence

II. MATERIALS AND METHOD

The materials used include;

- 1. **DC Micro-grid Model:** Comprising photovoltaic (PV) generation, battery energy storage system (BESS), and a DC link bus.
- 2. **EV Fast Charging Station:** Modeled as a nonlinear, high-power DC load with Level-3 charger, up to 50-350 kW connected directly to the micro-grid.
- 3. **STATCOM:** Modeled as a voltage-sourced converter (VSC) with an interfacing transformer and DC capacitor.
- 4. **Artificial Neural Network (ANN) Controller:** Designed to replace conventional PI control for STATCOM operation, providing adaptive regulation of reactive power and harmonic mitigation
- 5. **MATLAB/Simulink:** Used for modeling, simulation, and implementation of the ANN-based STATCOM controller.
- 6. **Neural Network Toolbox:** For training, validating, and testing the ANN controller

Method

A simulation-based approach was employed, integrating a DC micro-grid with renewable generation, battery storage, and EV fast charging followed by the design and implementation of a STATCOM equipped with an Artificial Neural Network (ANN)-based controller.

Volume 11, Issue 4, Jul-Aug-2025, ISSN (Online): 2395-566X

Description of Study Case Model

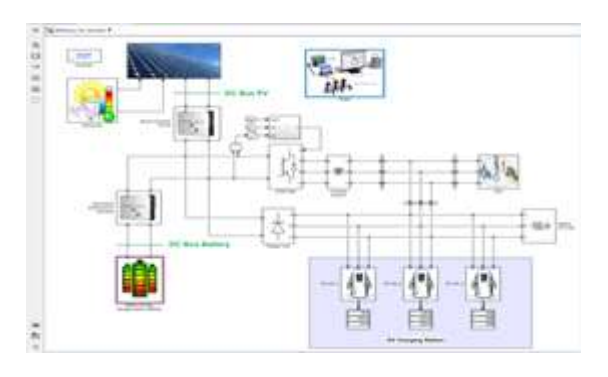


Figure 1: Simulink Model of a DC Microgrid Integrated with PV, BESS, EV Fast Charging Station, and STATCOM.

Figure 1 presents the Simulink model of a DC micro-grid integrating photovoltaic (PV) generation, a battery energy storage system (BESS), a Level-3 EV fast charging station, and a STATCOM for power quality enhancement. A 500 kW photovoltaic (PV) array serves as the primary renewable energy source, interfaced through a DC link that connects to both the STATCOM and other subsystems. A battery energy storage system (BESS) is integrated to support charging flexibility, mitigate renewable intermittency, and ensure stable DC bus voltage. The EV charging station consists of multiple Level-3 chargers supplying several electric vehicles simultaneously, modeled as high-power nonlinear loads that introduce harmonics and voltage fluctuations. The STATCOM is connected in shunt to the grid interface for voltage regulation and harmonic mitigation. The model captures the dynamic interaction between renewable energy sources, storage, and high-power EV charging demands, making it suitable for evaluating the performance of an ANN-controlled STATCOM in ensuring stable and reliable micro-grid operation.

Mathematical Model Solar Power Generation

The power output from the solar panels depends on solar irradiance, panel area, and efficiency. The power generated by the solar system at any time is given by

$$P_{PV}(t) = A*G(t)*\eta PV$$
 (1) Where;

P_PV (t): power generated by the photovoltaic system at time,

A: area of the solar panels (m2) G(t): solar irradiance at time t (W/m2) ηPV : efficiency of the photovoltaic system

Battery Storage

Battery energy storage is essential for stabilizing intermittent renewable generation from solar and wind. The battery's state of charge (SoC) changes based on the charging and discharging processes. The change in battery energy

$$SoC(t) = SoC(t-1) + \frac{\eta_{charge} * P_{charge}(t) - \frac{P_{discharge}(t)}{\eta_{discharge}}}{E_{bat}}$$
(2)

Where:

SoC(t): state of charge at time (t)

P_charge (t): power used to charge the battery (W)

P_discharge (t): power discharged from the battery (W)

 η_charge and $\eta_\text{discharge}$: efficiencies for charging and

discharging the battery E_bat: battery capacity

Utility Grid

Grid interaction for a distributed generation (DG) system can be modeled by considering both the power exported to the grid and the power imported from the grid. If renewable generation is low and battery could not meet the load demand, then the power deficiency is purchased. The imported power from the grid is given by

$$P_{grid}^{imp} = min\left(P_d(t) - P_{pv}(t) - P_w(t) - P_b^{out}(t)\right) \tag{3}$$

ilarly, if the total generation from renewable sources and batteries exceeds the load demand, the surplus power is exported. The exported power to the grid is given by

$$P_{grid}^{exp} = max \left(P_{pv}(t) + P_w(t) + P_b^{out}(t) - P_d(t) \right) \tag{4}$$

Where

P d (t): total power demand at time

P_pv (t): power from Solar PV Generation

P w (t): power from wind Generation

P_b^out (t): ower Supplied by the Batte

STATCOM Design

Voltage-sourced converter-based STATCOM was modeled for reactive power compensation and harmonic mitigation.

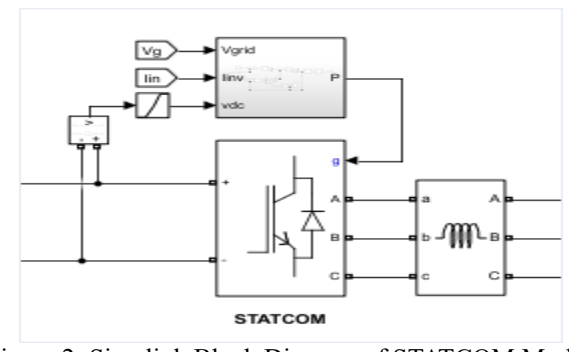


Figure 2: Simulink Block Diagram of STATCOM Model

Current Compensation

The shunt active filter injects current to compensate for the reactive and harmonic component s of the load current. The

source current should ideally be free of harmonic and reactive components.

$$I_{inj} = L_L - I_s \tag{5}$$

By applying Kirchhoff's voltage Law

$$I_{s} = I_{L} + I_{inj} \tag{6}$$

DC Link Voltage

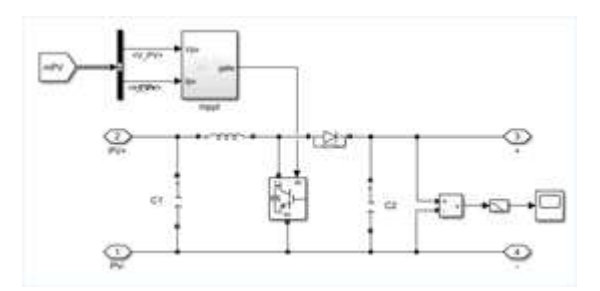


Figure 3: Simulink Block Diagram of DC Link Voltage Boost Converter

DC voltage is given by $V_{dc} = \sqrt{2} * V_{LL} * k$

Where

V LL: line to line rms voltage

k: safety factor typically ranging from 1.1 to 1.5

DC Link Capacitor

DC link capacitor is given by

$$C_{dc} = \frac{2P}{V_{dc}^2 * \omega * \Delta V_{dc}} \tag{8}$$

Where

P: load active power

Vdc: dc link voltage

 ΔV_{dc} : voltage ripple (20V)

 ω : angular frequency

DC Link Inductance

The shunt active filter inductor value is given by

$$L_{sh} = \frac{\sqrt{2}*V}{2\pi*f_{sw}*\Delta I} \tag{9}$$

Where

V: rms line voltage

 f_{sw} : switching frequency (10kHz)

 ΔI : allowable ripple current (5A)

Total Harmonic Current Distortion (THDc)

$$THD_{c} = \frac{\sqrt{I_{2}^{2} + I_{3}^{2} + I_{4}^{2} + I_{5}^{2} \dots + I_{n}^{2}}}{I_{1}} \times 100\%$$

$$I_{rms} = \sqrt{I_{2}^{2} + I_{3}^{2} + I_{4}^{2} + I_{5}^{2} \dots + I_{n}^{2}}$$

$$Crest Factor = \frac{|I_{peak}|}{I_{rms}}$$

$$(12)$$

$$I_{rms} = \sqrt{I_2^2 + I_3^2 + I_4^2 + I_5^2 \dots + I_n^2}$$
 (11)

$$Crest Factor = \frac{|I_{peak}|}{I_{rms}} \tag{12}$$

 I_i is the amplitude of the i^{th} harmonic,

 I_l is that for the fundamental component

Design of ANN Controller

The Artificial Neural Network (ANN) controller is employed to regulate the operation of the STATCOM, enabling adaptive voltage support, harmonic mitigation, and reactive power compensation in the DC microgrid under varying load conditions imposed by EV fast charging.

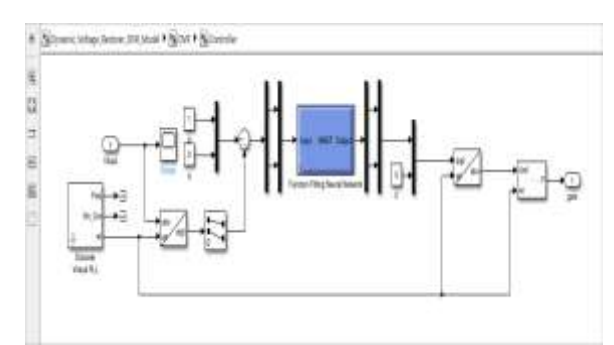


Figure 4: Simulink Block of ANN STATCOM Controller

ANN Training

(7)

When a neural network is trained for a specific task, the process begins by comparing the network's predicted output with the actual target output. The difference between these two values is quantified using an error function, which serves as a measure of accuracy. The main objective of training is to minimize this error so that the network produces predictions that closely match the desired output. By iteratively adjusting the internal weights and connections, the network gradually improves its ability to process inputs and deliver accurate results.

Beyond minimizing errors, the training process also enables the neural network to learn and adapt. This adaptability allows the network to recognize patterns, generalize knowledge, and apply it to new or unseen inputs. In doing so, the system develops the capability to solve complex problems across different domains, from classification and prediction to decision-making. The general architecture of a neural network, showing the flow of data through input, hidden, and output layers, is presented in Figure 5

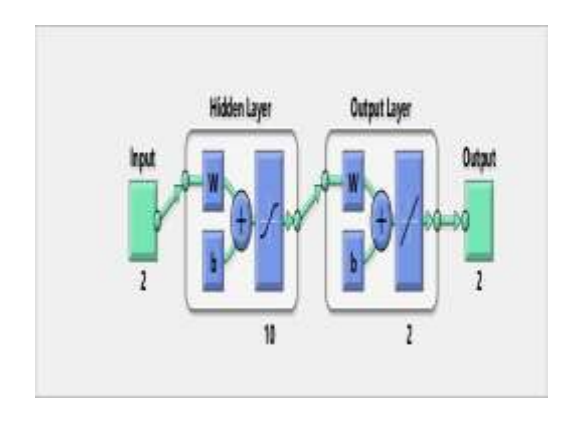


Figure 5: Neural Network Structure

The input received by the neurons is given by
$$Input(x) = [x_i]$$
 (13)

The Initialize weights and bias of the ANN structure is giving

$$w = [w_1 \ w_2], [b] \tag{14}$$

The neurons sum all the signals it receives, with each signal being multiplied by its associated weights on the connection. The weighted sum of the output node i is giving by

$$F_{i} = \left(\begin{bmatrix} w_{1} & w_{2} \end{bmatrix} \times \begin{bmatrix} x_{1i} \\ x_{2i} \end{bmatrix} \right) + b$$

$$F_{i} = \left\{ (w_{1} \times x_{1i}) + (w_{2} \times x_{2i}) \right\} + b$$
(15)
(16)

$$F_i = \{ (w_1 \times x_{1i}) + (w_2 \times x_{2i}) \} + b \tag{16}$$

Calculated output is given by

Ouput
$$(y_i) = \emptyset(F_i)$$
 (17)

$$(y_i) = \emptyset[(w_1 \times x_{1i}) + (w_2 \times x_{2i})] + b$$
 (18)

$$\emptyset(yi) = \left(\frac{1}{1+e^{-\nu_i}}\right) \tag{19}$$

$$\begin{aligned}
\text{Output } (y_i) &= \emptyset(F_i) \\
(y_i) &= \emptyset[(w_1 \times x_{1i}) + (w_2 \times x_{2i})] + b \\
\emptyset(yi) &= \left(\frac{1}{1 + e^{-v_i}}\right) \\
(y) &= \frac{1}{1 + e^{-((w_1 \times x_{1i}) + (w_2 \times x_{2i}) + b)}}
\end{aligned} (17)$$

Where

 x_{1i}, x_{2i} : inputs received by neurons

 w_{1i} , w_{2i} : weights of the neurons

b_i: is the neuron threshold.

Ø= activation function (Tan Sigmoid Function)

Fi = weighted sum of the output node i

 e_i =error in node i

y_i: is the output that passes through a sigmoid transfer function that is normally non-linear to give the final output.

III. RESULT AND DISCUSSION

Figure 6 illustrates the power profiles of the major components within the DC micro-grid during the simulation. The PV output power (Ppv) initially peaks at about 2000kW, then declines to around 1200 kW at 1.5 s before recovering toward 1700 kW by the end of the interval. The battery (Pbat) dynamically responds by charging up to approximately +500kW when surplus PV power is available and discharging down to about -400kW when PV generation drops, thereby balancing the system.

The STATCOM (PSTATCOM) maintains a nearly constant active power around 2000 kW, confirming its primary function of voltage regulation and reactive power support rather than active power variability. Meanwhile, the grid power (Pgrid) remains stable, fluctuating slightly around 500-700kW, which demonstrates that the coordinated operation of PV, BESS, and STATCOM reduces stress on the grid while ensuring stable supply for the EV fast charging station.

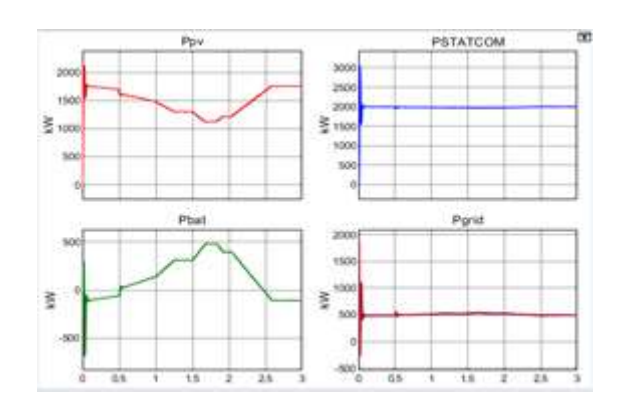


Figure 6: Power Profiles of PV, STATCOM, BESS, and Grid in the DC Micro-grid under EV Fast Charging Conditions

Figure 7 shows the power demand profiles of the EV fast charging units and the static load connected to the DC microgrid. EV Charger 1 (P EV_1) maintains a steady demand of about 600 kW, while EV Charger 2 (P_EV_2) operates close to 480 kW throughout the simulation. EV Charger 3 (P EV 3) records a relatively lower but stable demand of approximately 250 kW. In parallel, the static load (P Static Load) remains constant at around 500 kW, indicating baseline consumption independent of EV charging dynamics. Together, these profiles highlight the high and sustained power demand imposed by Level-3 EV fast charging stations on the micro-grid, reinforcing the necessity of coordinated energy management with BESS and ANN-controlled STATCOM to ensure voltage stability, minimize grid stress, and maintain power quality under continuous heavy loading.

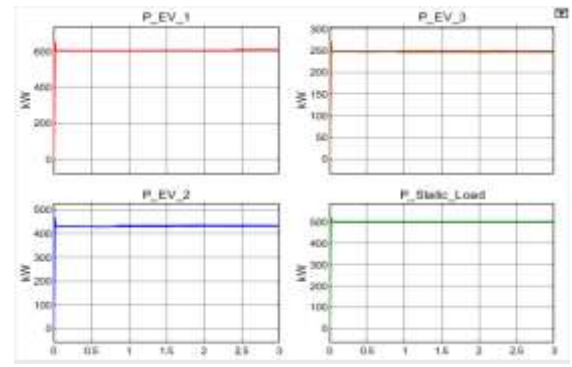


Figure 7: Power Demand Profiles of EV Charging Units and Static Load in the DC Microgrid

Figure 8 illustrates the harmonic current distortion introduced at the point of common coupling (PCC) by the EV fast charging station. The observed waveform deviates from the ideal sinusoidal shape of the fundamental frequency due to the presence of multiple harmonic components. Such distortions are typical in nonlinear loads like fast chargers, where highpower converters interact with the grid. According to the IEEE 519-2022 standard for low-voltage systems (≤1.0kV), the

permissible individual harmonic distortion should remain below 5%, while the total harmonic distortion (THD) should not exceed 8%. Exceeding these limits can lead to overheating of equipment, reduced power quality, and overall inefficiency in the micro-grid, underscoring the importance of effective compensation strategies such as the ANN-controlled STATCOM used in this study.

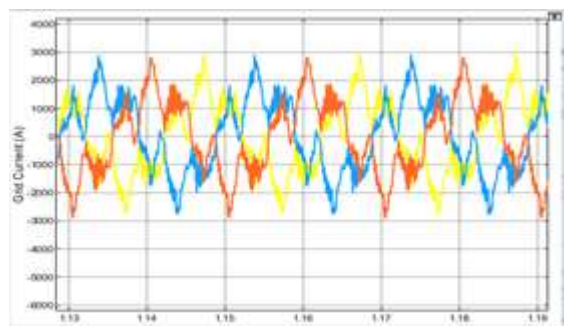


Figure 8: Shows Injected Harmonic Current Waveform

Figure 9 presents the harmonic spectrum order injected at the point of common coupling (PCC) in the power system network. The spectrum clearly indicates the presence of dominant odd harmonics, particularly at the 11th and 13th orders, which significantly distort the current waveform. The computed total harmonic distortion (THD) at the PCC is 14.05%, exceeding the IEEE 519-2022 standard limit of 8% for medium-voltage systems. This violation highlights the adverse impact of EV fast charging stations on power quality and emphasizes the necessity of advanced mitigation techniques, such as ANN-controlled STATCOM, to maintain compliance with regulatory standards and ensure stable microgrid operation.

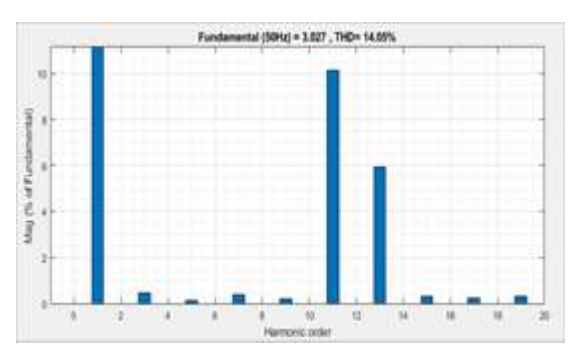


Figure 9: Shows Order of Harmonic Current Spectrum

Figure 10 shows the current waveform at the point of common coupling (PCC) after the installation of the STATCOM for harmonic mitigation. With the ANN-controlled STATCOM in operation, the previously dominant 11th and 13th harmonics introduced by the EV fast charging station were effectively eliminated. As a result, the current waveform is significantly smoother and closer to the ideal sinusoidal profile, demonstrating the capability of the STATCOM to restore power quality and ensure compliance with IEEE 519-2022 standards.

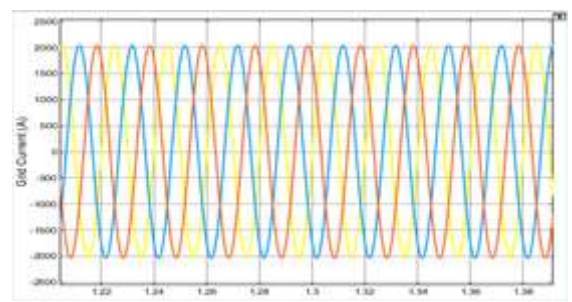


Figure 10: Shows Current Waveform after STATCOM Installation

Figure 11 presents the harmonic spectrum obtained from FFT analysis after the installation of the STATCOM. The results reveal a remarkable improvement in power quality, with the total harmonic distortion (THD) at the PCC reduced to just 1.23%, well within the IEEE 519-2022 compliance limits. Specifically, the dominant harmonics observed earlier were almost completely suppressed, with the 11th-order component reduced to 0.01% and the 13th-order reduced to 0.15%. Compared to the uncompensated case where the THD reached 14.05%, this represents a reduction of over 90%, clearly demonstrating the effectiveness of the ANN-tuned STATCOM controller in mitigating harmonic distortion caused by EV fast charging, restoring waveform integrity, and ensuring stable and reliable micro-grid operation.

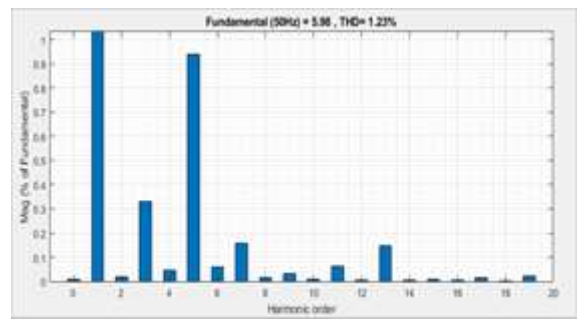


Figure 11: Shows Order of Harmonic Current Spectrum after STATCOM Installation

Figure 12 illustrates the performance plot of the mean square error (MSE) against the number of iterations (epochs), providing insight into the effectiveness of the ANN training process. The blue curve corresponds to training results, the green curve to validation results, and the red curve to test results. As training progresses, the MSE is calculated at each epoch, and the optimal point is identified where the three curves nearly coincide, signifying the best generalization of the model. At this stage, further training is unnecessary, as it could lead to overfitting and reduced prediction accuracy. A closer look at the plot reveals that the best validation performance was achieved at epoch 20, with a minimized error of 0.0034611, indicating a well-trained model capable of delivering accurate predictions for STATCOM control in the DC microgrid

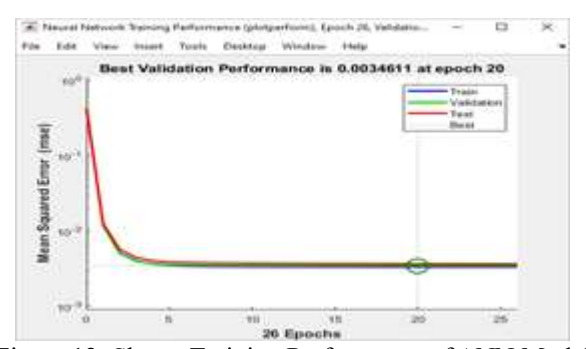


Figure 12: Shows Training Performance of ANN Model

Figure 13 presents the regression plot, which evaluates the fitness of the ANN training outputs against the actual target data obtained from the PI controller. In the plot, the dashed line represents the ideal target (perfect fit), while the solid line shows the best linear regression between the predicted outputs and the targets. In regression analysis, an R-value of 1 indicates a perfect linear relationship, while an R-value of 0 suggests no correlation. As shown in the figure, the obtained R-value of 0.9879 demonstrates an excellent correlation, confirming that the proposed ANN controller achieved a near-perfect mapping between inputs and outputs. This high regression accuracy validates the effectiveness of the training, testing, and validation processes, thereby reinforcing the ANN controller's robustness and reliability for harmonic mitigation in the EV fast charging station

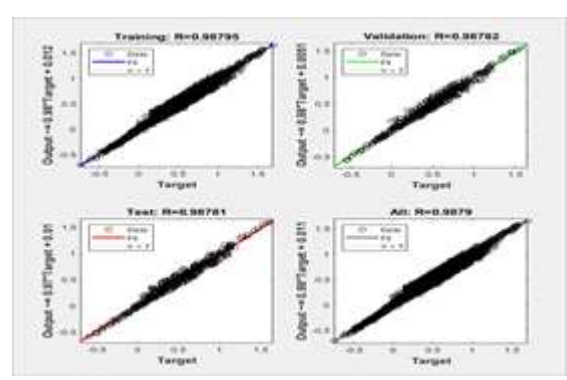


Figure 13: Shows Fitness of Training Data

IV. CONCLUSION

This study advances the field of intelligent control for DC microgrids with electric vehicle (EV) fast charging integration. While STATCOMs are well established for voltage regulation and harmonic mitigation, their performance has traditionally relied on proportional integral (PI) controllers, which are limited in handling nonlinear and rapidly varying conditions. This work introduces an Artificial Neural Network (ANN)-based STATCOM controller, specifically designed for DC micro-grids with Level-3 EV fast charging, providing enhanced adaptability, robustness, and dynamic response. The study also

examine energy management and power quality independently, areas often treated separately.

Through ANN-controlled STATCOM operation, the research demonstrates simultaneous improvements in voltage stability, harmonic suppression, and power flow optimization. Furthermore, a comprehensive simulation framework incorporating renewable energy sources (RES), energy storage systems (ESS), and fast charging stations has been developed, offering a platform for further investigation into micro-grid resilience and intelligent compensation strategies. Based on these contributions, several recommendations are proposed.

Future research should explore hybrid intelligent control approaches, such as ANN combined with fuzzy logic or reinforcement learning, to further enhance performance under uncertain EV charging conditions. Hardware-in-the-loop (HIL) validation and small-scale experimental prototypes are also recommended to establish practical feasibility. For industry, the adoption of ANN-controlled STATCOMs can mitigate voltage instability and power quality deterioration in EV charging networks. Policymakers should incentivize the integration of renewable energy and advanced compensation technologies into EV infrastructure to enable sustainable and low-carbon transport electrification.

REFERENCE

- 1. Altin, N., Eyimaya, S. E., & Nasiri, A. (2023). Multiagent-based controller for microgrids: An overview and case study. Energies, 16(5), 2445.
- 2. Bianchi, G., & Medici, V. (2017). PID control for distributed generation systems: Applications and limitations. IEEE Transactions on Power Systems, 32(3), 2154–2165.
- Fubara, I. & Ijeoma, R.C. (2019). Investigating the Reliability and Viability of Embedded Generation to Improve the Power Supply (Eleme, Rivers State as a Case Study), IOSR Journal of Engineering (IOSRJEN), 09(08): 27-37.
- Hong, J., Yin, J., Liu, Y., Peng, J., & Jiang, H. (2019). Energy management and control strategy of photovoltaic/battery hybrid distributed power generation systems with an integrated three-port power converter. IEEE Access, 7, 82838–82847.
- 5. Huang, X., & Tang, Y. (2017). Optimization-based control for distributed generation: Genetic algorithms and particle swarm optimization approaches. Renewable Energy, 105, 250–263.
- 6. Ijeoma R.C. & Olisa I.E. (2019). Design of 3phase50hz 500kva 33/0.4kv Distribution Substation, IOSR Journal of Electrical and Electronics Engineering (IOSR-JEEE) 14(4) Ser.1: 38-48.



Volume 11, Issue 4, Jul-Aug-2025, ISSN (Online): 2395-566X

- 7. Ijeoma, R.C. (2025c). Transformative Energy Practices and Innovations: A Path towards Global Energy Equity. SustainE. 1(2).1-11. doi:10.55366/suse.v1i2.14
- 8. Ijeoma, RC., & Odu, EV., (2025a). Future Load Energy Forecast of Stone-City, Mgbede Community Rural Electrification Scheme. International Journal of Science, Engineering and Technology (IJSET); 13(3), 1-9
- Ijeoma, RC., & Odu, EV., (2025b). Power System Surges: Causes, Effects, and Mitigation Strategies. International Journal of Science, Engineering and Technology (IJSET); 13(3), 10-17
- 10. Liu, Y., & Li, W. (2019). Sliding mode control for power regulation in distributed generation systems with renewable energy sources. IEEE Transactions on Sustainable Energy, 10(1), 178–189.
- 11. Madueme, T. C., & Kalu, E. E. (2015). Artificial neural network applications in power system stability and reliability analysis. International Journal of Electrical Power & Energy Systems, 64, 179-190.
- 12. Mir Nahidul Ambia, Hasanien, H. M., Al-Durra, A., & Muyeen, S. M. (2015). Harmony search algorithm-based controller parameters optimization for a distributed-generation system. IEEE Transactions on Power Delivery, 30(1), 246–255.
- 13. Mohan, B., Subramanian, K., & Rao, V. (2019). Feedforward neural networks and backpropagation learning: A review and implementation. Journal of Intelligent & Fuzzy Systems, 36(5), 4517–4528.
- 14. Mwasilu, F., & Ojo, O. (2024). Robust MIMO controller for distributed generation system-based grid-tied voltage sourced converter. 2024 IEEE Energy Conversion Congress and Exposition (ECCE), 833–840.
- 15. Pan, D., & Wang, H. (2018). Adaptive control techniques for variable renewable energy generation in distributed systems. International Journal of Electrical Power & Energy Systems, 99, 562–573.
- 16. Razmi, D., & Lu, T. (2022). A literature review of the control challenges of distributed energy resources based on microgrids (MGs): Past, present and future. Energies, 15(13), 4676.
- 17. Shravani Chapala, N., Narasimham, R. L., Ram, T., & Lakshmi, G. S. (2023). PV and wind distributed generation system power quality improvement based on modular UPQC. 2023 International Conference on Advanced & Global Engineering Challenges (AGEC), 82–87.
- 18. Tuan, N. T., & Wang, Z. (2018). Fuzzy logic control for power flow regulation in hybrid distributed generation systems. Journal of Renewable and Sustainable Energy, 10(5), 054301.
- 19. Zhang, R., & Wang, J. (2019). Application of unified power quality conditioner in renewable energy-based distributed generation systems. Energy Conversion and Management, 187, 456–470.
- 20. Zhao, L., & Xu, M. (2019). Model predictive control for real-time power optimization in hybrid distributed

- generation systems. IEEE Transactions on Smart Grid, 10(2), 2310–2321.
- 21. Zhou, P., & Yu, X. (2020). Hybrid control strategies for distributed generation: A combination of fuzzy logic, PID, and model predictive control techniques. Electric Power Components and Systems, 48(5), 432–448.
- 22. Zhou, X., & Zhang, Y. (2020). Voltage source converter-based control for grid-connected distributed generation systems. Journal of Electrical Engineering & Technology, 15(3), 487–501